

An Optimal Structure for a 34-Meter Millimeter-Wave Center-Fed BWG Antenna: The “Cross-Box” Concept

K. L. Chuang

Ground Antenna and Facilities Engineering Section

This article presents a new approach to the design of the planned NASA/JPL 34-m elevation-over-azimuth (Az-El) antenna structure at the Venus site (DSS-13). The new antenna structural configuration accommodates a large (2.44-m) beam waveguide (BWG) tube centrally routed through the reflector-alidade structure, a unique elevation wheel design, and an optimal structural geometry. The new design encompasses a “Cross-Box” elevation wheel–reflector base substructure that preserves homology while satisfying many constraints, such as structure weight, surface tolerance, stresses, natural frequency, and various functional constraints. The functional requirements are set to ensure that microwave performance at millimeter wavelengths is adequate.

The new Cross-Box configuration was modeled, optimized, and found to satisfy all DSN HEF baseline antenna specifications. In addition, the new structure design was conceptualized and analyzed with an emphasis on preserving the structure envelope and keeping modifications relative to the HEF antennas to a minimum, thus enabling the transferability of the BWG technology for future retrofitting. Good performance results were obtained.

I. Introduction

The DSN is planning to build a new R&D antenna at the Venus Deep Space Tracking Station (DSS-13) at Goldstone, California [1]. The proposed R&D antenna is intended to perform as a test bed for the development of advanced telecommunication technologies, among which are the incorporation of (1) beam waveguide optics, (2) Ka-band (32 GHz) components, and (3) high gain/noise temperature capability in the millimeter wavelength range.

The inclusion of a BWG system is viewed as an item of high research priority [2] for the existing baseline design of the 34-m HEF network (Figs. 1 and 2). It is also proposed that any new designs be capable of retrofit to the existing network of antennas at low cost and that all future DSN antennas make use of the BWG optics.

The modeled Cross-Box configuration presented in this article is one of several options that satisfy the above conditions while introducing minimal changes in the antenna geometry

and tipping structure weight relative to present 34-m DSN HEF antennas. The new design also maintains the major features of existing drive systems for the Az-El mount, the alidade structure, and the azimuth wheel and track. Proper design of the elevation wheel and support structure (ELWH) obviates the need to redesign the main reflector and its backup truss (REFL). Thus, optimal configuration of the antenna structure primarily entails the design of the substructure that transfers loads from the main reflector to the elevation bearings only (Fig. 2)—herein called substructure ELWH. This article describes the design approach and finite element model formation.

II. Design Statement

The “Cross-Box” design was modeled as a truss-type structure with all joints (nodes) modeled as pinned joints. Connectivity between nodes can be achieved with bars/rods (one-dimensional elements) or with plates (triangular or quadrilateral). All elements are assumed to be non-bending members. Altogether, there are approximately 3900 members and 1200 nodes in the whole antenna structure above the azimuth track. For optimization purposes, the members are judiciously grouped to maintain antenna symmetries, resulting in 207 groups of design variables for the problem. The design variables comprise bar areas and plate thicknesses.

Determination of the sizes of the members is the eventual problem that must be solved. Optimization schemes to obtain explicit solutions are available in the literature for structures in general [3]–[10] and for antennas in particular [11]. Not as easily resolved are problems of establishing optimal configurations, especially those in which path obstructions are encountered in the structural geometry. The major difficulty in designing for the present antenna is of this nature. Discussion on the course taken to overcome it will be emphasized. The complexities of the real antenna structure geometry and component fabrication do not readily lend themselves to simple solutions. Shape optimization schemes may help but they are mostly of the perturbation type [12]–[18]. Effectively, this amounts to perturbation of nodes in a finite element model. However, attempting to weave a tube of eight-foot diameter within the antenna structure demands more than minor adjustments in geometry. By and large, when solution strategies exist, they are usually problem-specific [12], [19]–[23]. Variational methods [23] are not applicable to structures of highly noncontiguous domain and therefore are of no value in the present problem. Although the layout theory propounded in [19]–[22] is applicable to 1- and 2-dimensional problems, it is extremely difficult to apply to 3-dimensional problems. Nevertheless, it is unlikely that any configuration under optimization will evolve into a dramatically different geometry

without creating other problems, such as overlapping/intersecting members.

When a viable configuration is found, the problem is “reduced” to one that is amenable to classical treatment of feasibility, Lagrange multipliers, Kuhn–Tucker conditions, etc. For larger problems, indirect methods are used whereby the notion of active and passive constraints is introduced. Optimality criteria methods [4]–[11] are based on such principles. Optimal member sizes for the Cross-Box antenna were obtained through the use of NASA/JPL–IDEAS programs [11], which employ a version of the optimality criteria methods [9]. The Cross-Box design antenna has more than 11,700 degrees of freedom, which is common for antennas of this size. Stiffness matrix decomposition time is significant and is compounded when designing the parabolic surface of the antenna. Attempts have to be made to best-fit thousands of points of the reflector surface to a paraboloid at different antenna elevations [26].

Another problem arises from the degree of statical indeterminacy of the structure. The more statically indeterminate the structure is, the harder it is to predict the inputs for the next iteration [9]. The methodology becomes sensitive to step-size/move limits chosen in the iterations. Not only does it take longer to converge on a solution but it is also possible for the algorithm to fail to yield a reasonable solution. In addition, other solution-strategy-dependent features may affect computational efficiency. Perhaps the most direct impositions come from side constraints. They increase computational time, if nothing else. At worst, these constraints might be such that the problem will have no feasible solution. The following are the dominant constraints that affect the design of the Cross-Box antenna:

- (1) Maximum allowable member stresses (yield and buckling).
- (2) Upper and lower bounds of member sizes.
- (3) Maximum allowable displacements at worst elevation angle:
 - (a) Surface distortion (rms) from a best-fit paraboloid due to gravity loading.
 - (b) Surface distortion (rms) from a best-fit paraboloid due to worst case wind (120 degrees elevation and 0 degrees azimuth) loading.
- (4) Boresight error due to worst case wind (0 degrees elevation and 120 degrees azimuth) loading.
- (5) Weight of tipping structure limited to 220 ± 10 percent kips.
- (6) Lowest natural frequency.

- (7) Survivability of antenna in stow position (at zenith) for a 100 mph wind.

Other less quantifiable constraints on conceptualizing the configuration are as follows:

- (1) The structure shall be such that an elevation range of 6 to 90 degrees is possible.
- (2) The structure shall be designed around the space required by the BWG path (as dictated by BWG optics) within the antenna structural domain.

The structure should also have the following attributes:

- (1) A simple configuration geometry.
- (2) Minimal member connections/joints.
- (3) Low-cost fabrication techniques.
- (4) Duplicability of substructures and symmetries.
- (5) Duplicability and retrofittability of the configuration to the existing DSN HEF antenna (this also implies that the design can adopt components from existing antennas).

These attributes will directly translate into reduced cost impact on the design.

III. Model Formation

To reach an optimum configuration for the antenna structure, steps were taken following the schematic of Fig. 3. The blocks indicate the end products while the arrow paths denote actions. In general, the design optimization strategy involves the following procedures:

- (1) Conceive modularization/substructuring.
- (2) Design and optimize each substructure.
- (3) Synthesize the antenna by assembling individually optimized substructures, followed by optimization of the antenna as a whole using results obtained in (2) as the best input prediction.

The above idealization assumes that the synthesis of optimum substructures will yield an optimum global structure through proper choice of modularization. Each procedure will now be described.

A. Modularization

In designing the antenna structure, some modularization is advantageous because it

- (1) Allows the problem to be more easily managed.
- (2) Allows the problem modules to be tackled separately and simultaneously—and thus more efficiently.
- (3) Allows individual modules to be solved on microcomputers, thus requiring less time on a “large” program run on a “large” computer.
- (4) Allows the convenience of making changes to, and testing of, individual modules without having to run the whole program/antenna structure.
- (5) Allows different degrees of difficulty encountered in different substructures to be treated by specialized programs. (For example, the NASTRAN program analyzes structures with bending members but NASA/JPL-IDEAS does not. On the other hand, the latter performs structural optimization and also surface best-fitting, which the former does not.)
- (6) Allows reduced mass storage.

The 34-m antenna at hand is divided into three substructures: (1) the main reflector and its backup truss, subreflector, and mount (REFL); (2) the elevation wheel structural assembly (ELWH); and (3) the alidade (ALD). They are distinguished by their distinct structural functions as shown in Fig. 2. The REFL module upholds a parabolic surface, allowing minimal surface distortion from some parabolic (shaped) profile, maintaining homology [24], and promoting symmetrical displacement of surface points. The ELWH module transfers loads (gravity and wind) from the REFL module to the ALD module and simultaneously counterbalances the REFL about the elevation axis. When the antenna is at zenith position, the ELWH module ideally provides a plane surface on which the REFL can be placed. When the antenna is at the horizon position, the ELWH, with the counterweight that it carries, balances the REFL, thus relieving the elevation drive from load bearing. The elevation drive is the only other point besides the two elevation bearings at which there is contact between the tipping structure and the alidade.

The third substructure, ALD, bears all the loads from the tipping structure transmitted through the elevation bearings. It provides the azimuth range for the antenna driven on a track. It also provides a mount for the elevation drive. Proper design of the antenna adheres to the principles described in [25].

B. Substructure Design and Optimization

The REFL module design of the NASA/JPL HEF antennas was kept intact: it consists of a parabolic reflector with radial ribs, hoops, and supporting truss. It is a symmetric structure as shown in Fig. 4. For a Cassegrain-type antenna, the secondary reflector and its quadripod mount are included in the REFL

design. The unique features of the new Cross-Box antenna come from the ELWH module with its homology features [24], [25].

The conceptualization of the ELWH design is based on the following observations and reasoning:

- (1) Eight points (on the circumference of a circle) forming the vertices of an octagon are selected at the base of the REFL substructure (Fig. 5). These are attachment points of the REFL to the ELWH enabling uniform displacement of the REFL under symmetric zenith loading. An octagonal truss system is conceived to be part of the ELWH where these attachments are enabled (Fig. 6).
- (2) Loads on the tipping structure must eventually be borne by the two elevation bearings. This implies that connections must be made from eight points to two points. However, this cannot be done directly if uniform deflection of the REFL is to be maintained under uniform zenith loading. Reactions at the eight points cannot be identical unless both points lie along the zenith axis. This is not allowed, however, because a BWG system is to be centrally routed. The solution to this problem is achieved by transferring the loading first to four points (four corners of a square) and then to two points.
- (3) The elevation wheel (bullgear) lies in the Y-Z plane perpendicular to the elevation axis (a line joining the two elevation bearings). It must be incorporated into the ELWH substructure and must exert even loading on the four points in (2). An elevation "axle" and the elevation wheel suggest that a "+" structural form is needed in the ELWH substructure.

Although an elevation "axle" is needed, BWG optics requirements demand that an eight-foot-diameter (2.44 m) path along the elevation axis be devoid of any structure. This means that a box must be built up to assume an elevation axle. Furthermore, to satisfy the criteria in (3), a cross-box must be constructed. This gives rise to the "Cross-Box" design. Figure 7 shows the position of the Cross-Box in relation to the octagonal truss. The "square" mentioned in (2) is dictated by nodes 9, 10, 11, and 12. Bracing members are not shown in Fig. 7. Elevation bearings are a radius distance from the center of the octagon and two feet below the lower edge of the truss. The box is tapered, with the thickest possible section at the central portion. This design feature ensures that flexural deflection of the "axle" is minimized. Figure 8 shows the complete envelope of the cross-box and the BWG path. Bracings for all faces (except 9-10-11-12-9, 25-26-27-28-31-32-21-22-25, and the four faces typified by 31-30-46-31) are not shown. Bar elements are grouped according to their symmetry about the X-Z

or Y-Z plane in conjunction with their positions. The cross-sectional thickness (of the tapered portion) of the x-direction leg of the Cross-Box is limited by the vertical section of the BWG path.¹ This design enables an elevation range of 6 to 90 degrees. Also, the elevation wheel (bullgear) is attached to the 8 points: 41, 23, 24, 42, 43, 29, 30, and 44. It has symmetry about both the X-Z and Y-Z planes and has a design similar to that of the DSN HEF antennas.

The transfer of loads from the REFL to the ELWH is done by connecting bar members from the octagonal truss to the cross-box. Figure 9a shows a plan view of how the connection is done. The "X" bracings shown are conceived to restrain relative rotation about the reflector local Z-axis between the cross-box and the octagonal truss. Note that the four points on the X-Z plane are equally loaded for Z-loading. Members symmetrical about the X-axis and those about the Y-axis are grouped differently to allow homology of structure. This allows for reduced RMS distortion due to Y-direction loading which creates an antisymmetric displacement pattern. Next, rigidity of the box structure is ensured by bracings as shown in Fig. 9b. The "X" bracing indicated by the broken lines in the center indicates that it is at the bottom face; the top face is open for the BWG path. Torsional rigidity of the cross-box about the local Z-axis is established by the bracing shown in the "eye view." The broken circle shows the vertical portion of the BWG tube.¹

The REFL substructure is optimized by restraining the eight attachment points from translation in all directions. The Rigging-Angle Method [26] was used to determine the worst root-mean-square distortion and pointing error (angle) of the best-fit parabolic surface. (The Rigging Angle Method determines the elevation angle for which, if a perfect paraboloid is designed, the worst distortion rms from a paraboloid will occur identically at the zenith and horizon looks of the antenna.) The following results were achieved:

- (1) Surface rms distortion from a best-fit paraboloid due to gravity loading alone is 0.005 inch.
- (2) Surface rms distortion from a best-fit paraboloid due to wind at 30 mph (120 degrees elevation and 0 degrees yaw) is 0.009 inch.
- (3) Boresight error due to a 30 mph wind (0 degrees elevation and 120 degrees yaw) is 0.003 degree.

These results depict the individual effect of the loads applied independently. Optimal sizing of the members has resulted in satisfying specifications as shown in Table 1.

¹Actually, this segment of the BWG tube is not vertical but tilted at an angle of 13.5 degrees to the vertical in the Y-Z plane.

An ALD substructure design can be constructed with little modification from the baseline antennas. Construction of ALD poses no difficulties since the only loadings are applied forces and moments at the elevation bearings. Performance characteristics similar to those of the DSN antennas were obtained with little modification in the design.

C. Substructure Synthesis and Optimization

Figure 10 shows a sketch of an assembled cross-box antenna. Note how the elevation wheel is attached to the components discussed in Figs. 7 and 8. Also seen are the tapered legs of the cross-box and the octagonal truss. The baseline antenna's structural envelope is preserved. Hence, the condition of the fewest changes possible to antenna subsystems is observed. Figures 10 and 11 show essentially the synthesized structure and its accommodation of a center-fed BWG system as dictated by microwave optics.

Optimization was performed on the antenna structural model combining REFL and ELWH. Member sizes in the REFL were not allowed to change (thus allowing direct usage of the DSS 15 design). Results obtained after optimization on member sizes satisfy all specifications. Table 1 lists performance indices achieved. Also cited are the DSN HEF antenna specifications.

IV. Summary

This article reveals the new Cross-Box design concept proposed for the planned 34-m-diameter development antenna at the Venus site. The proposed design has the accommodability of a large beam waveguide (2.4-m) system for Ka-band operability and retrofittability to the 34-m high efficiency antennas. The Cross-Box antenna is optimal in both structural configuration and member size, satisfying many functional constraints. Observance of structural compatibility with the 34-m antennas allows transferability of technologies.

Acknowledgment

The author would like to thank Smoot Katow, John Cucchissi, and Dr. Roy Levy for their helpful suggestions. Dr. Fikry Lansing offered much encouragement and support throughout this work.

References

- [1] J. G. Smith, "Proposed Upgrade of the Deep Space Network Research and Development Station," *TDA Progress Report 42-88*, vol. October–December 1986, Jet Propulsion Laboratory, Pasadena, California, pp. 158–163, February 15, 1987.
- [2] R. C. Clauss and J. G. Smith, "Beam Waveguides in the Deep Space Network," *TDA Progress Report 42-88*, vol. October–December 1986, Jet Propulsion Laboratory, Pasadena, California, pp. 174–182, February 15, 1987.
- [3] L. Schmit and H. Miura, "Approximation Concepts for Efficient Structural Synthesis," NASA CR-2552, March 1976.
- [4] N. Khot, L. Berke, and V. Venkayya, "Comparison of Optimality Criteria Algorithms for Minimum Weight Design of Structures," *AIAA Journal*, vol. 17, pp. 182–190, February 1979.
- [5] S. Segenreich, N. Zouain, and J. Herskovits, "An Optimality Criteria Method Based on Slack Variables Concept for Large Scale Structural Optimization," in *Proceedings of the Symposium on Applications of Computer Methods in Engineering*, School of Engineering, University of Southern California, pp. 563–572, August 1977.
- [6] L. Berke and N. Khot, "Use of Optimality Criteria Methods for Large Scale Systems," in *Proceedings of the AGARD Symposium on Structural Optimization*, AGARD Lecture Series No. 70, pp. 1–29, October 1974.
- [7] C. Fleury, "An Efficient Optimality Criteria Approach to the Minimum Weight Design of Elastic Structures," *Computers and Structures*, vol. 2, pp. 163–173, 1980.
- [8] V. B. Venkayya, N. S. Khot, and L. Berke, "Application of Optimality Criteria Approaches on Automated Design of Large Practical Structures," in *Proceedings of the Second Symposium on Structural Optimization*, Milan, Italy, pp. 3.1–3.19, 1973.
- [9] R. Levy and W. Parzynski, "Optimality Criteria Solution Strategies in Multiple-Constraint Design Optimization," *AIAA Journal*, vol. 20, no. 5, pp. 708–715, April 13, 1981.
- [10] E. J. Haug and J. S. Aurora, *Applied Optimal Design*, New York: John Wiley, 1979.
- [11] R. Levy and R. J. Melosh, "Computer Design of Antenna Reflectors," in *Proceedings of ASCE 99*, pp. 2269–2285, November 1973.
- [12] K. Wasserman, "Three-Dimensional Shape Optimization of Arch Dams with Prescribed Shape Functions," *Journal of Structural Mechanics*, vol. 11, no. 4, pp. 465–489, 1983–84.
- [13] A. Francavilla, C. V. Ramakrishnan, and O. C. Zienkiewicz, "Optimization of Shape to Minimize Stress Concentration," *J. of Strain Analysis*, vol. 10, no. 2, pp. 63–70, 1975.
- [14] O. C. Zienkiewicz and J. S. Campbell, "Shape Optimization and Sequential Linear Programming," in *Optimum Structural Design*, R. H. Gallagher and O. C. Zienkiewicz (eds.), New York: John Wiley, pp. 109–126, 1973.
- [15] M. E. Botkin and J. A. Bennett, "Shape Optimization of Three-Dimensional Folded Plate Structures," presented at the 25th Structures, Structural Dynamics, and Materials (SDM) Conference, Palm Springs, California, 1984.

- [16] S. D. Rajan and A. D. Belegundu, "A Shape Optimization Approach Using Fictitious Loads as Design Variables," presented at the 28th Structures, Structural Dynamics, and Materials (SDM) Conference, Monterey, California, 1987.
- [17] "The Optimum Shape: Automated Structural Design," an international symposium sponsored by General Motors Research Laboratories, Warren, Michigan, October 1985.
- [18] E. J. Haug, K. K. Choi, J. W. Hou, and Y. M. Yoo, "Shape Optimal Design of Elastic Structures," presented at the International Symposium on Optimum Structural Design, University of Arizona, Tucson, Arizona, 1981.
- [19] G. I. N. Rozvany, "A General Theory of Optimal Structural Layouts," presented at the International Symposium on Optimum Structural Design, University of Arizona, Tucson, Arizona, 1981.
- [20] G. I. N. Rozvany and R. D. Hill, "A Computer Algorithm for Deriving Analytically and Plotting Structural Layout," *Comp. and Struct.*, vol. 10, pp. 295-300, 1979.
- [21] G. I. N. Rozvany, C. M. Wang, and M. Dow, "Prager-Structures: Arch-Grids and Cable Networks of Optimal Layout," *Comp. Meth. Appl. Mech. Engrg.*, vol. 31, 1982.
- [22] W. Prager and J. E. Taylor, "Problems of Optimal Structural Design," *Journal of Appl. Mech.*, vol. 35, no. 1, pp. 102-106, 1968.
- [23] J. P. Zolesio, "Domain Variational Formulation for Free Boundary Problems," *Optimization of Distributed Parameter Structures*, E. J. Haug and J. Cea (eds.), Sijthoff & Noordhoff, Alphen aan den Rijn, The Netherlands, pp. 1165-1208, 1981.
- [24] S. Von Hoerner, "Homologous Deformations of Tilttable Telescopes," in *Proceedings of the ASCE*, pp. 461-485, October 1967.
- [25] S. Von Hoerner, "Design of Large Steerable Antennas," *The Astronomical Journal*, vol. 72, no. 1, February 1967.
- [26] R. Levy, "A Method for Selecting Antenna Rigging Angles to Improve Performance," *Deep Space Network Space Programs Summary 37-65*, vol. II, Jet Propulsion Laboratory, Pasadena, California, pp. 72-76, July 1970.

Table 1. Achieved performance indices

Antenna type	Weight (kips)	RMS distortion due to gravity alone (inches)	RMS distortion due to 30 mph wind: worst case (inches)	Boresight error due to 30 mph wind: worst case (mdeg)
Cross-box antenna	244	0.009	0.009	10
DSN HEF antenna	217	0.015	0.019	13*

*This figure includes the alidade. A figure for the tipping structure alone was not available. From this estimate, the alidade contribution is approximately 4 millidegrees.

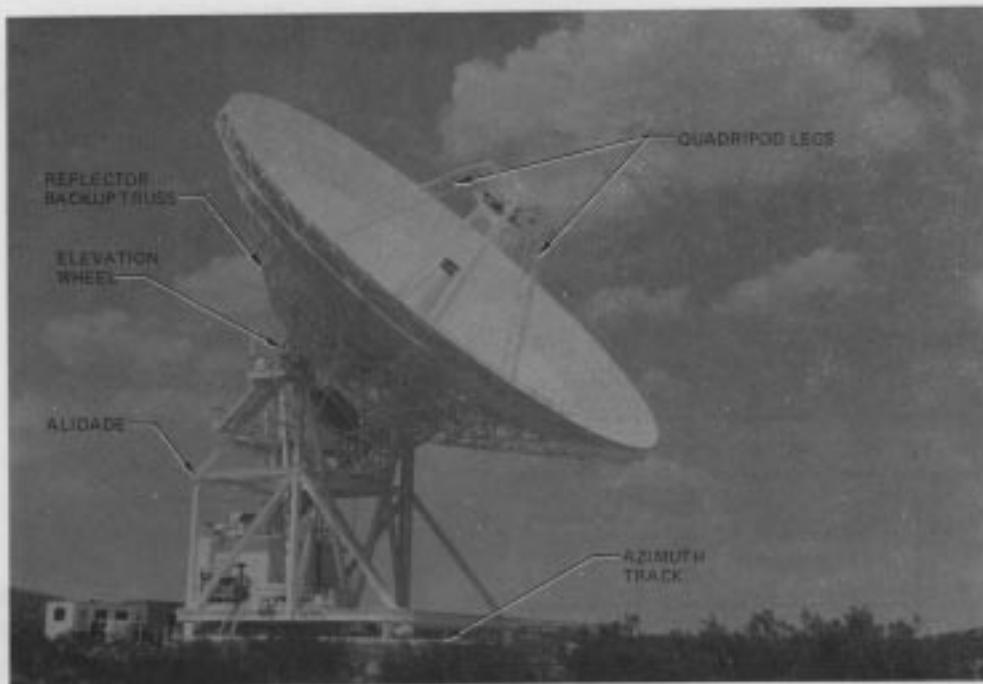


Fig. 1. NASA DSN HEF antenna at Goldstone, California (two identical antennas are located in Spain and Australia)

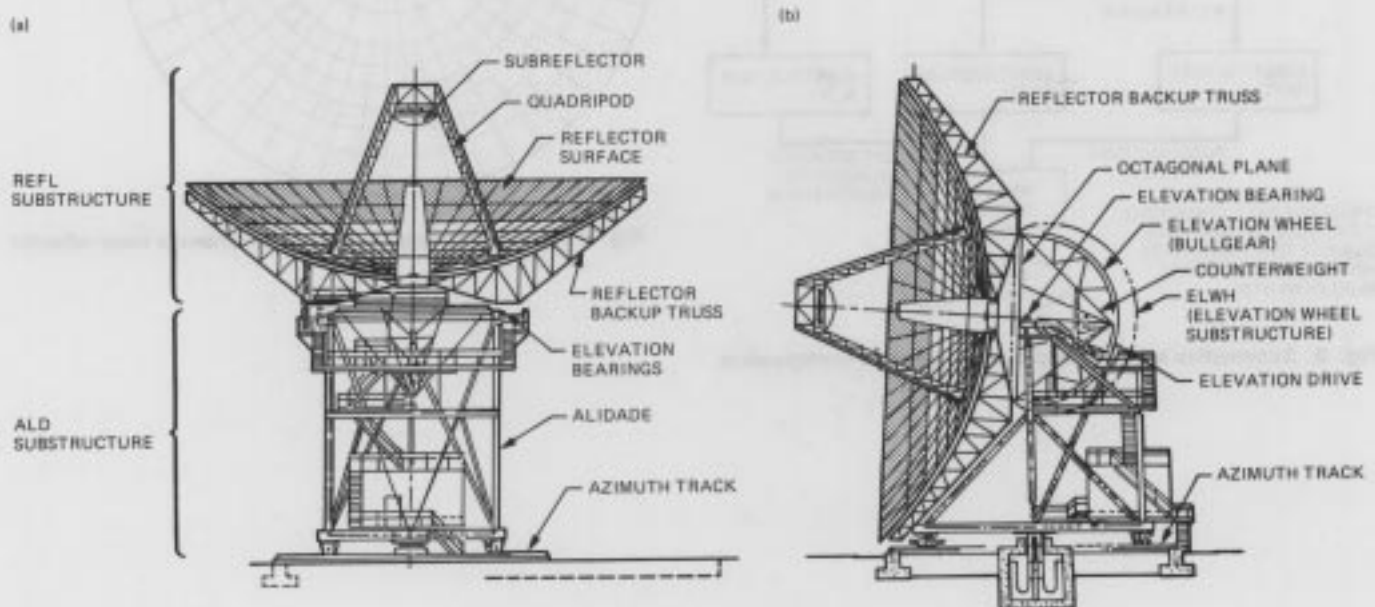


Fig. 2. NASA DSN HEF 34-m antenna (a) at zenith position and (b) at horizontal position

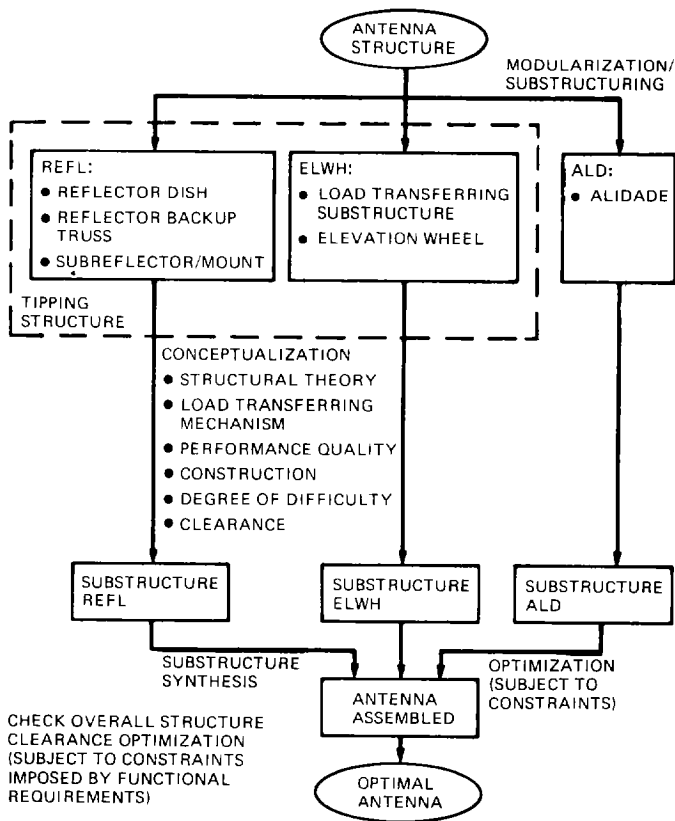


Fig. 3. Schematics showing approach to antenna configuration

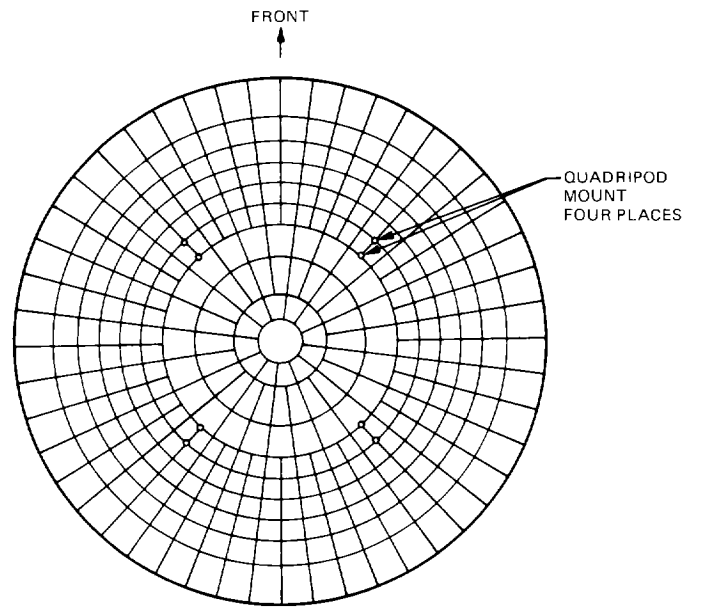


Fig. 4. Front surface of the 34-m HEF antenna main reflector

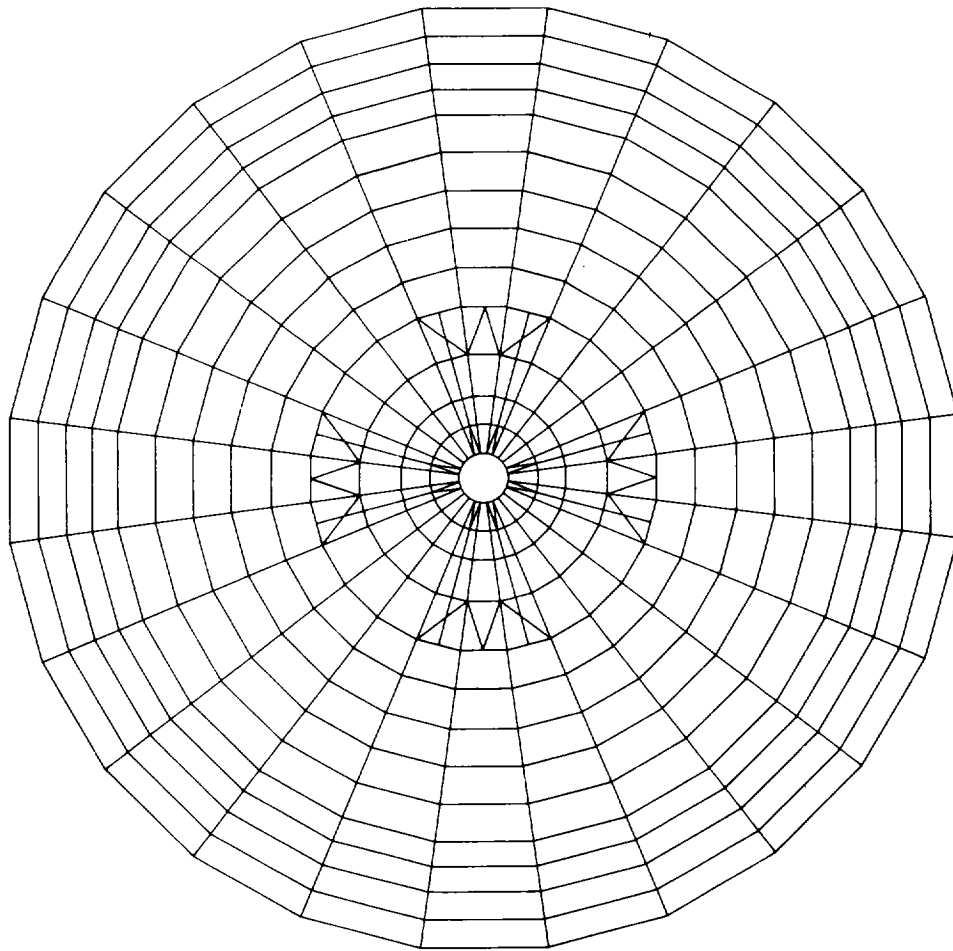


Fig. 5. Finite element model of the reflector (back) showing eight points where attachment of REFL and ELWH will occur

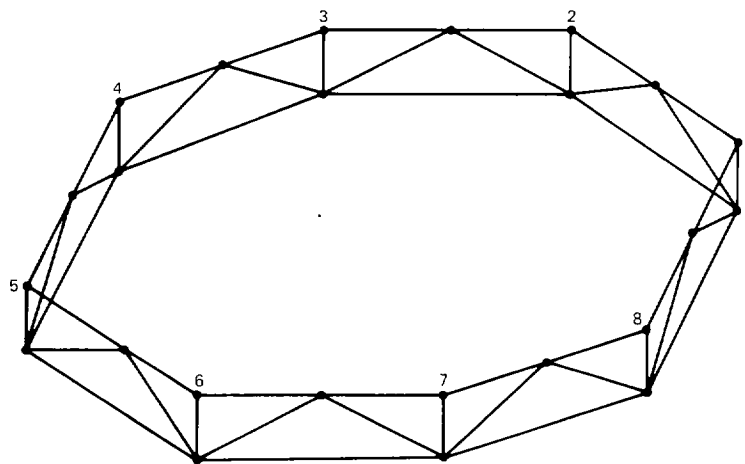


Fig. 6. The octagonal truss

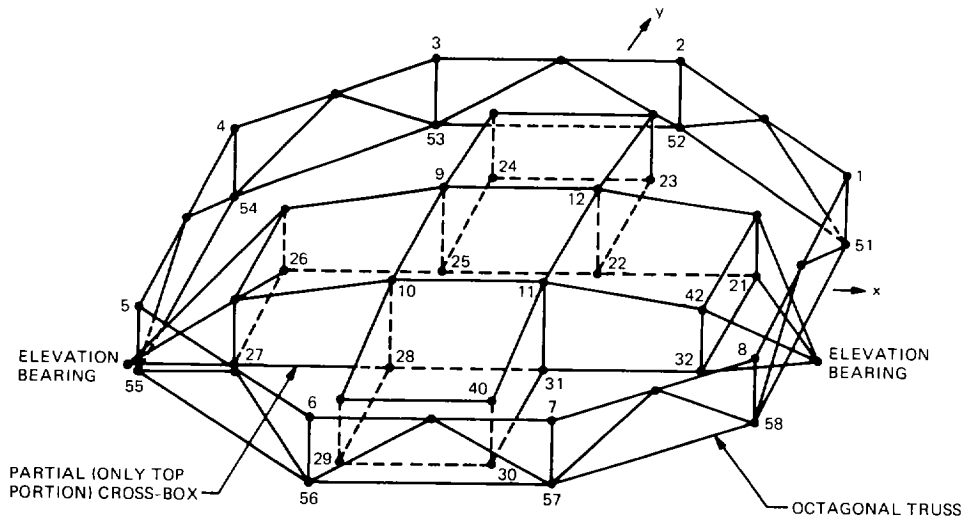


Fig. 7. The cross-box concept showing relative position of cross-box to octagonal truss

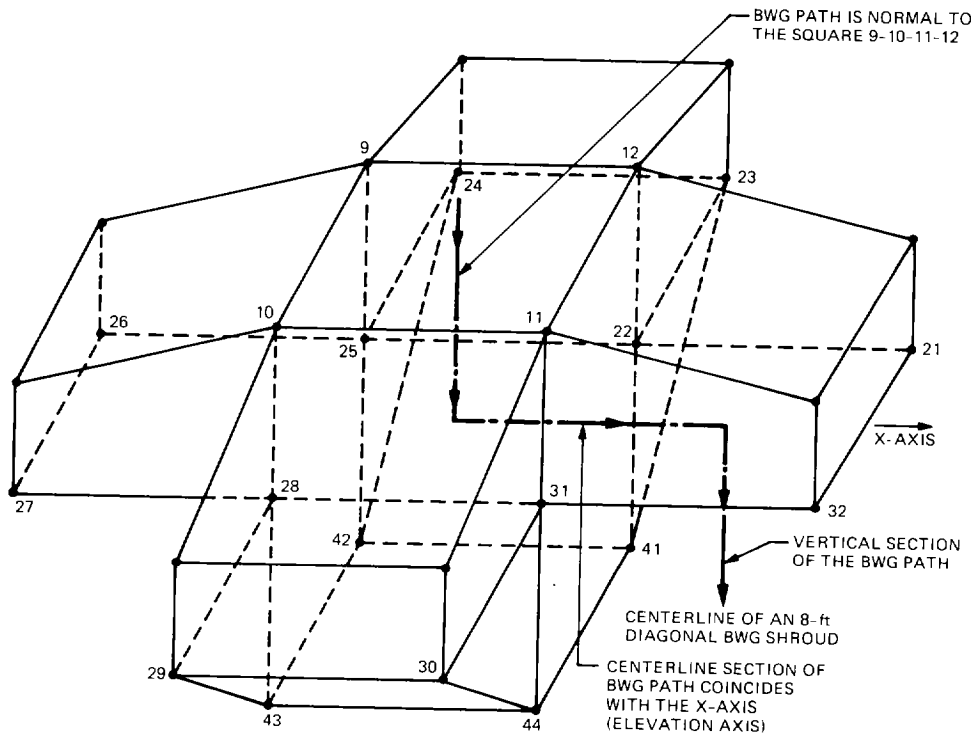


Fig. 8. Center piece (cross-box) showing BWG path

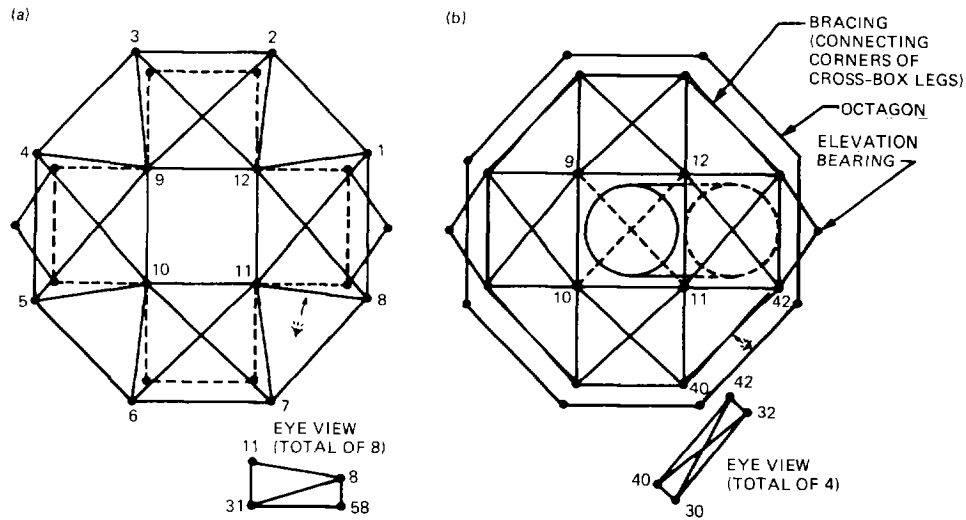


Fig. 9. Connection of bar members from octagonal truss to cross-box: (a) view emphasizing connecting links; (b) view emphasizing cross-box bracing

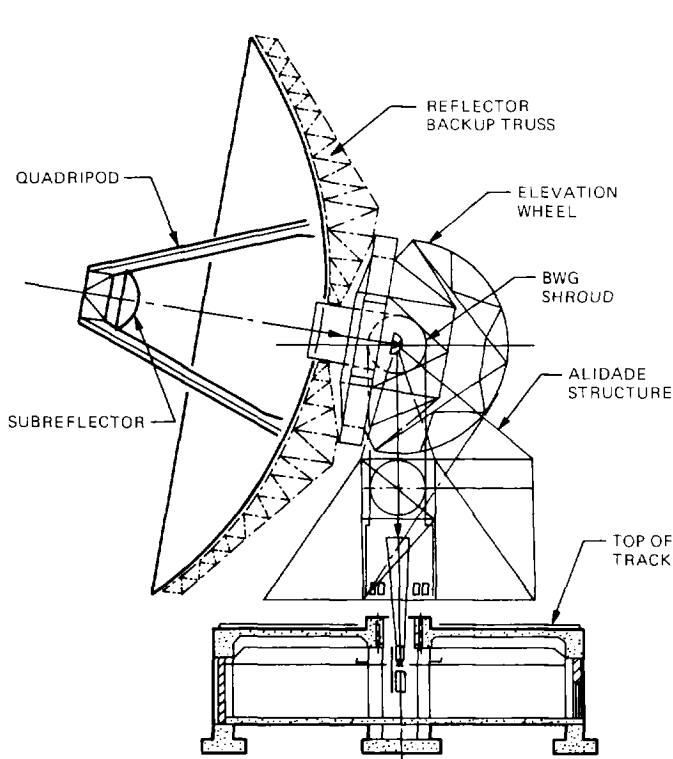


Fig. 10. Approximate relative position and dimension of BWG path to the antenna (Y-Z plane)

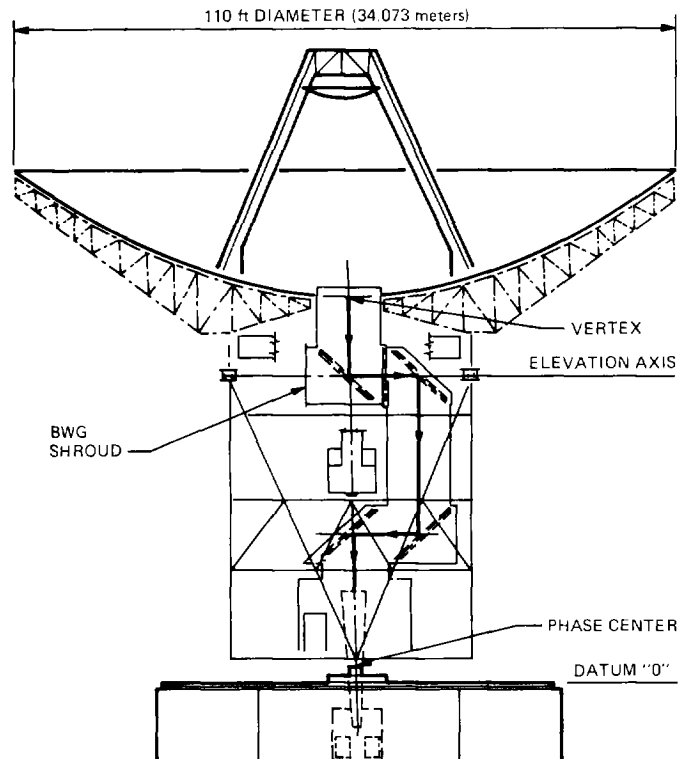


Fig. 11. Approximate relative position and dimension of BWG path to the antenna (X-Z plane)